Green Chemistry

Accepted Manuscript

ROYAL SOCIETY OF CHEMISTRY

www.rsc.org/greenchem

Carbon dot–hemoglobin complex-based biosensor for cholesterol detection

*Trang Thi Bui and Soo-Young Park**

School of Applied Chemical Engineering, Polymeric Nano Materials Laboratory, Kyungpook National University, Daegu 41566, Republic of Korea

*Corresponding author E-mail: psy@knu.ac.kr

Abstract: In the present study, a carbon dot/hemoglobin (CD/Hb) complex is used as a bio-receptor in an optical cholesterol biosensor. This optical sensor detects cholesterol through fluorescence enhancement of CD, which is normally quenched via π-π interactions between CD and Hb in the CD/Hb complex. CD is released from the CD/Hb complex because hydrophobic interactions between Hb and cholesterol are more favorable than π-π interactions between CD and Hb. The CD/Hb complex enabled selective detection of cholesterol within a linear range from 0 to 800 μM, with a limit of detection of 56 μM and a response time ≤ 5 minutes, and in human blood plasma. Compared with other cholesterol sensors, the CD/Hb complex-based biosensor is simple, highly sensitive, selective, rapid, eco-friendly, and cost-effective for cholesterol detection in both biological and environmental samples.

Keywords: cholesterol, cholesterol optical biosensor, fluorimetry, carbon dots, hemoglobin

Introduction

Cholesterol is a fatty substance produced by the liver that is also found in food. It acts as a precursor of steroid hormones, vitamin D, and bile [1]; however, it is essential to maintain cholesterol levels within a certain range in the human body. The concentration of cholesterol in human serum should be lower than 200 mg/dL under normal circumstances, and any serum level which is higher than 240 mg/dL indicates high blood cholesterol. High cholesterol levels can cause damage to blood vessels and result in cardiovascular diseases [2]. Several methods have been employed to detect cholesterol, such as electrochemical methods, thin layer chromatography, high-performance liquid chromatography, optical methods, and polarographic assays [3-10]. However, these methods have limitations, such as lacking selectivity or specificity, requiring complex methods or processes, and long reaction times. The most common method used to detect cholesterol is the electrochemical method, which is limited owing to its complex setup requiring a three-electrode system [3-8]. In

addition, most cholesterol sensors use cholesterol oxidase (ChO), a cholesterol enzyme, which is expensive and can be easily denatured [6-10].

In recent years, fluorescence methods have attracted the attention of many researchers in the biosensing field because of its ease, high sensitivity, rapid implementation, and low cost [11]. However, most cholesterol optical sensors are less sensitive and relatively more complicated, because an optical transducer is required, such as hydrogel polymer matrices [12], metal complexes (ruthenium II, Ru) [13], or quantum dots from heavy metals (e.g., CdSe) [14], to which cholesterol is immobilized. In addition, the dyes and heavy metals used as optical transducers are harmful to researchers and hazardous to the environment [15, 16]. Thus, novel safe fluorescence materials are required. Since their discovery in 2004, carbon dots (CD) have become a popular class of carbon nanomaterials, and several hundreds of studies on the unique construction and characteristics of CD have been reported [17]. Fluorescent CD has been widely used in bio-imaging, cell-labeling, and sensing because of its non-toxicity, eco-friendliness, high fluorescence, biocompatibility, and fast response times [18, 19]. Zeng et al. reported that DNA could be readily identified when added to a CD/methylene blue complex solution [20]. CD has also been used for the detection of glucose [21], dopamine [22], glutathione [23], and phytic acid [24] in recent years. These developments are based on exploiting the "off-on" fluorescence property of CD. CD is quenched or turned "off" when receptors such as metal ions or bio-compounds (which contain a conjugate system) are absorbed onto the CD surface. Adsorption is mediated through several interactions such as through π-π interactions (van der Waals forces), metal catechol interactions, and oxidation–reduction following a photo-induced electron transfer (PET) or electron transfer quenching mechanism. CD is enhanced or turned "on" when a more favorable complex between the analyte and conjugate (or metal ion) formed [20-25].

Hemoglobin (Hb) is a tetrameric protein containing four heme prosthetic groups, with each polypeptide chain containing one heme group (Figure SI 1a). In the blood, Hb carries oxygen from the respiratory organs to the rest of the body. The heme group in Hb has a conjugated structure with an iron II atom at the center and four porphyrin N atoms arranged at the corners of the face [1]. Via this conjugated structure, the heme group in Hb can interact with CD through π–π interaction, quenching CD fluorescence. In addition to the four heme groups, Hb also contains four polypeptide chains that can non-specifically absorb compounds with hydrophobic moieties (e.g., cholesterol) via hydrophobic interactions. Hydrophobic interaction is thermodynamically more stable than π–π interaction [26]. Thus, these two interactions can be exploited for biosensing. A hydrophobic analyte can be detected via a more favorable hydrophobic interaction with Hb,

disrupting the extant π-π interaction between Hb and CD, and enhanced CD fluorescence. Given that cholesterol has hydrophobic moieties, as shown in Figure SI 1b, we hypothesized that a new cholesterol biosensor could be designed based on the CD/Hb complex and these competitive interactions.

In this work, we report for the first time that cholesterol can be detected by the CD/Hb complex through fluorescence enhancement. Fluorescence quenching and enhancement were achieved by complexation between Hb and CD, and addition of cholesterol to the CD/Hb aqueous complex solution, respectively. This CD/Hb complex-based biosensor is simple, highly sensitive, selective, rapid, eco-friendly, and cost-effective for cholesterol detection. Therefore, the proposed CD/Hb complex has the potential to be applied as a practical blood cholesterol sensing platform.

Materials and methods

Materials: Citric acid (CA, 99.5%), glucose, cholesterol, L-ascorbic acid, human Hb (lyophilized powder), human serum (plasma), horseradish peroxidase (HRP), and a dialysis tube (typical molecular weight cut-off = 14,000 Da) were purchased from Sigma-Aldrich (USA). Metal salts (NaCl, KCl, $FeCl_2$, $MgCl_2$, and $CuCl_2$), ethylene diamine (EDA, 99.5%), and ethanol (99.8%) were obtained from Duksan, Korea. Deionized (DI) water was used for all experiments. All reagents of analytical grade were used directly without further purification.

Instrumentation: CD was prepared using a mini bench-top reactor (Parr series 4560, Parr. Co, USA) and its size was measured using dynamic light scattering (DLS, Zeta sizer Nano-ZS90, Malvern, UK) with laser light at a wavelength of 633 nm. Data shown represent the average from three independent measurements of a 0.002 mg/mL CD solution. The UV-Vis, photoluminescence (PL), and Fourier transform-infrared (FT–IR) spectra were recorded on a UV-2401 PC spectrophotometer (Shimadzu, Japan), RF-5301 PC (Shimadzu, Japan), and Jasco FT/IR–620 spectrometer (KBr method, Jasco, Japan), respectively. Large molecules in plasma blood were removed by centrifuge (V1512-Vision, V3000i, Vision scientific.Co.LTD, Korea). Photographs of CD, CD/Hb, and the CD/Hb/cholesterol solutions were taken with a digital camera (Nikon D90, Nikon, Japan).

Preparation of CD: CD was prepared according to a previously reported method that was slightly modified to use with a mini bench-top reactor [27]. Briefly, CA (0.4 g) and EDA (270 µL) were dissolved in DI water (80 mL). Then, the mixed solution was transferred to a sealed reactor (200 mL) and heated at 200°C for 4 h. After

the reaction, the reactor was cooled to room temperature (20°C) in air. The product, which was brown-red and transparent, was subjected to dialysis to obtain pure CD. After dialysis, the final concentration of the CD solution was approximately 6.13 mg/mL, which was calculated from the solid weight after complete drying.

Preparation of the Hb/CD complex: The CD solution was diluted with DI water to obtain a 0.2 mg/mL stock solution. Various amounts of aqueous Hb solutions (10 μM) and DI water were added to the CD solution (50 μM, 0.2 mg/mL) in 5 mL tubes to obtain a final concentration of 0.002 mg/mL of the CD solution with different final Hb concentrations (C_{Hb}). The fluorescence of CD/Hb aqueous solutions were measured with a fluorescence spectrophotometer using an excitation wavelength at 380 nm. The complexation of CD with other materials (such as Hb, HRP, lysozyme, L-ascorbic acid, urea, Cu^{2+}, Na^{+}, Fe^{2+}, Fe^{3+}, Mg^{2+}, and glucose) was investigated at the same final concentration of 8 μM.

Detection of cholesterol: In a typical assay, the CD (0.002 mg/mL)/Hb (6 μM) complex was prepared in 5 mL tubes using stock CD (0.2 mg/mL) and stock Hb solutions (10 μM). Then, different amounts of cholesterol stock solutions (1 mg/mL) were added to the CD/Hb complex to determine the linear range of cholesterol detection. The cholesterol stock solution was prepared by the following method. First, cholesterol powder (0.01 g) was dissolved in ethanol (1 mL), and then diluted with DI water (9 mL) to obtain a 1 mg/mL cholesterol solution. To investigate the selectivity of cholesterol detection, various aqueous biocompound (such as glucose, galactose, L-ascorbic acid, and urea) solutions were added to the CD/Hb complex solution (5 mL) to obtain the same final concentration of 800 μM. All experiments were repeated in triplicate at 20°C.

For assays involving human serum, blood plasma (Sigma-Aldrich) was centrifuged at 10,000 rpm (11,393 g) for 20 min to remove large molecules, and then dissolved in ethanol (99%) to make a stock solution before added to the CD/Hb complex solution. The cholesterol level in human blood plasma was independently determined through an enzymatic method with the ASAN Set Total-cholesterol Reagent (ASAN PHARM., Seoul, Korea).

Results and discussion

CD was synthesized from CA and EDA via hydrothermal carbonization treatment under high pressure at 200°C for 4 h (see Materials and methods). In this reaction, CA and EDA represent the raw carbon precursor

and the surface-doping reagent, respectively. The carbonization temperature of CA is low [28, 29], and its fluorescent yield increases under passivation of surface amine groups from urea, diamine, lysine, etc., which decreases the band gap due to increased electron density [30]. The reactions between the three acid groups of CA and two amine groups of EDA at hydrothermal conditions have been shown to induce high fluorescence with a wide range of emission wavelengths. Characteristic properties of CD derives from its unique structure, which contain aromatic rings and functional groups on the surface [31]. When complexation between CD and Hb occurs, the high CD fluorescence is quenched. Breaking the CD/Hb complex by adding cholesterol restores CD fluorescence due to the formation of more favorable hydrophobic interactions between Hb and cholesterol (Scheme 1). To characterize the ability of this biosensor to detect cholesterol, the structure, optical properties, and fluorescence response of CD and the CD/Hb complex with and without cholesterol were investigated.

Structural and optical properties of CD

The size distribution of CD was investigated by DLS (Figure 1a). The average size of CD was between 1.5 to 2 nm, indicating that monodisperse CD was successfully synthesized, consistent with reported data [27, 32]. Figure 1b shows the FT-IR spectrum of CD. Several characteristic absorption peaks caused by hydrothermal carbonization treatment of CD were observed at 2935–2868 cm^{-1} (CH anti-symmetric and symmetric stretching), 679 cm^{-1} (CH bending out-of-plane deformation), and 1637 cm^{-1} (vibration band of C=C and C=O stretching). Furthermore, the characteristic peaks of doping diamine were also observed at 1262 cm^{-1} (C-N stretching) and 3296–3386 cm^{-1} (N-H stretching). FT-IR data indicated that several functional groups were produced on the CD surface, such as amino (NH_2), hydroxyl (OH), and carboxyl groups (COOH). Based on its small size (from DLS) and multifunctional surface groups (from FT-IR), CD is likely compatible with various conjugated compounds and soluble in the hydrophilic solvents. The fluorescence properties of CD were investigated with UV-Vis and photoluminescence (PL) spectroscopy. The inset in Figure 1c shows photographs of the CD aqueous solution (0.001 mg/mL), which changed from clear to a light-blue color under UV (365 nm) light, demonstrating the fluorescence of CD. Figure 1c exhibits the UV-Vis and PL spectra (excited at 380 nm) of CD (0.002 mg/mL). In the UV-Vis spectrum, two central peaks at 210 nm and 340 nm, and a shoulder peak at 250 nm were observed. The sharp peak at 210 nm and the shoulder peak at 250 nm are ascribed to n-π* and π*-π* transitions of aromatic C=C bonds, respectively, whereas a large peak around 340 nm is attributed to an n-π* transition of functional groups (C=O, C=N bonds) on the CD surface [32, 33]. In the PL spectrum excited at 380 nm, a strong emission peak was observed at 450 nm, which is within the wavelength range of blue light (inset

Figure 1c). Figure 1d shows the normalized PL spectra at different excitation wavelengths. Because of its small size and multifunctional surface groups, CD is excited at different excitation wavelengths and emit across a wide color band, from blue to yellow green [18, 19, 31]. This fluorescence property is promising for cell labeling and bio-imaging applications [34].

Fluorescence quenching/enhancement of the CD/Hb complex solution with cholesterol

Complexation between CD and Hb was studied with fluorescence spectroscopy. As shown in Figure 2a and b, CD fluorescence was significantly quenched when Hb (6 μM) was added to 0.002 mg/mL CD solution. CD fluorescence (Figure 2a (i)) was reduced by 50% upon Hb complexation (Figure 2a (iii)), suggesting that π-π stacking (through van der Waals interactions) occurred between the aromatic ring system of CD and the heme group on Hb. The UV absorption spectra of CD and Hb (Figures 2c (i), (ii)) indicated that the energy absorption of CD (absorbance at 340 nm, 3.65 eV) was higher than that of Hb (absorbance at 404 nm, 3.01 eV), and the emission spectrum of CD excited at 380 nm (Figure 2c (iii)) overlapped with the absorption band of Hb (Figure 2c (ii)). These results suggest that fluorescence quenching occurs through a photoinduced electron transfer (PET) process wherein the heme group of Hb and the aromatic ring system of CD act as the acceptor and donor, respectively. Fluorescence quenching through the PET process was also shown to occur in a CD/metal ion complex [24]. To confirm whether quenching results from π-π interactions between the heme groups of Hb and aromatic rings of CD, lysozyme and HRP proteins (which contain polypeptide chains without and with only one heme group [compared to four in Hb], respectively) were added to a aqueous CD (0.002 mg/mL) solution to a final concentration of 8 μM. Figure 3 shows the log relative PL intensity values (log F_{CD}/F), where F_{CD} and F indicate CD PL intensities at 380 nm excitation before and after complexation, respectively. This ratio represents the degree of CD fluorescence quenching induced by the addition of the indicated compounds/biomolecules. Log (F_{CD}/F) values of Hb, HRP, and lysozyme were 1.19, 0.313, and -0.0350, respectively, demonstrating a correlation in the degree of fluorescence quenching and the number of heme groups per molecule. Metal ions such as Na^{+}, Mg^{2+}, Fe^{2+}, Cu^{2+}, and Fe^{3+} [24, 35] were also tested for fluorescence quenching at the same final concentration (8 μM). The log (F_{CD}/F) values of these metal ions were much smaller (-0.0191, -0.0249, 0.00791, 0.0122, and 0.0393, respectively) than that of Hb (1.19), because the electron densities of metal ions are lower compared to that of the heme group of Hb. Furthermore, common biomolecules, such as glucose, urea, and L-ascorbic acid, were also tested. Their log (F_{CD}/F) values were much smaller (0.00236, -0.0170, and -0.00790 for glucose, urea, and L-ascorbic acid, respectively) than that of Hb

(1.19), indicating that fluorescence quenching did not occur. Thus, Hb forms a complex with CD and quenches CD fluorescence through interactions with its heme group.

Cholesterol is amphiphilic with a hydrophilic hydroxyl group and hydrophobic alkyl chains (see Figure SI 1b). The hydrophobic alkyl chains of cholesterol tend to non-specifically interact with the hydrophobic patches of Hb via hydrophobic interactions. Cholesterol binding with Hb may disrupt the CD/Hb complex and restore CD fluorescence. Figures 2a (iv) and 2b (iii) show the fluorescence intensity of the CD/Hb complex (0.002 mg/mL and 6 μM, respectively) after the addition of cholesterol (400 μM). The fluorescence increased by 50%, suggesting that the Hb/cholesterol complex is thermodynamically more favorable than the CD/Hb complex. The energy of hydrophobic interactions is approximately 40 KJ/mol, which is 10 times higher than that of π-π interactions (van der Waals forces) (0.4–4.0 KJ/mol) [26]. As a control experiment, the fluorescence intensity of CDs did not change upon cholesterol addition (Figure 2a (ii)), indicating that cholesterol itself does not affect the fluorescence intensity of CD. Scheme 1 shows our model in which binding between cholesterol and Hb releases CD from the CD/Hb complex restoring CD fluorescence.

Detection of cholesterol by the CD/Hb complex

To optimize the CD/Hb complex for biosensor applications, various amounts of Hb (10 μM) and CD (50 μL, 0.2 mg/mL) were dissolved in DI water in 5 mL tubes to obtain different final concentrations (C_{Hb}). As shown in Figures 4a and b, the PL intensity of CD excited at 380 nm decreased gradually with increasing C_{Hb}. The degree of quenching increased rapidly as the C_{Hb} increased at low C_{Hb}, and then saturated with further increases of C_{Hb} (Figure 4b). Approximately 80% of the fluorescence intensity was quenched at C_{Hb} = 6 μM (Figure 4b). Thus, unless otherwise noted, we used final concentrations of 6 μM and 0.002 mg/mL for Hb and CD, respectively, in subsequent experiments with the CD/Hb complex. The time required to quench CD fluorescence intensity was also investigated. Figure 5 exhibits the change of F_{CD}/F as a function of time at C_{Hb} = 0.2 and 1.2 μM. Quenching of CD fluorescence saturated within 90 s after adding Hb at both C_{Hb} tested, indicating that CD/Hb complex formation occurs rapidly within 2 min.

Performance of the CD/Hb sensor

The dynamic range of cholesterol (C_{cho}) detection by the CD/Hb complex was evaluated. Figure 6a and b show the fluorescence spectra (excited at 380 nm) of CD/Hb/cholesterol solutions at different C_{cho} and a plot of log $F_{CHC}/F_{CD/Hb}$ (where $F_{CD/Hb}$ and F_{CHC} indicate PL intensities before and after loading cholesterol

solutions, respectively) as a function of C_{cho}, respectively. The fluorescence of CD in the CD/Hb complex was progressively enhanced as C_{cho} increased, and the log $F_{CHB}/F_{CD/Hb}$ value increased linearly with an increase in C_{cho} by the following equation ($r^2 = 0.990$):

$$\mathrm{Log}\left(\frac{F_{CHC}}{F_{CD/Hb}}\right) = 1.95.10^{-4}C_{cho} + 0.0115$$

in which C_{cho} was in the range of 0-800 μM (0–30.9 mg/dL) and the limit of detection (LOD) was estimated to be 56 μM [36]. To the best of our knowledge, the linear range was comparable to that of previously described cholesterol sensors, and the LOD was comparable to or lower than that of previously described cholesterol sensors (see Table SI 1). This linear range is also suitable for medical applications [2].

The selectivity of the CD/Hb complex to cholesterol was tested with L-ascorbic acid, galactose, urea, and glucose, which are basic biomolecules found in human serum. Figure 7 shows the log ($F_{bio}/F_{CD/Hb}$) values with different biomaterials, where $F_{CD/Hb}$ and F_{bio} are the PL intensities before and after adding biomaterials, respectively, at the same final concentration of 800 μM. Only cholesterol resulted in fluorescence enhancement, whereas the other biomolecules resulted in further fluorescence quenching. These biomolecules are hydrophilic, rendering interactions with Hb difficult in water. Thus, competitive π-π and hydrophobic interactions among CD, Hb, and cholesterol provide a new foundation for the development of an optical cholesterol sensor platform with high sensitivity and selectivity. Because the speed of detection and pH are important factors to consider for biosensor development, we evaluated the performance of the CD/Hb complex focusing on these parameters. Figure 8a shows the fluorescence of CD/Hb complex solutions as a function of time after adding cholesterol (600 μM). The fluorescence intensity saturated within 5 min, which is suitable for biosensor applications. Figure 8b shows a plot of the log ($F_{CHC}/F_{CD/Hb}$) as a function of pH. The $F_{CHC}/F_{CD/Hb}$ ratio was similar across the pH range from 6.4 to 7.2, indicating that this biosensor can be used with human serum under physiological pH conditions.

Finally, we tested the ability of the CD/Hb complex to detect cholesterol in human plasma serum. The original amount of cholesterol in human serum was determined independently with a different method as described in the Materials and Methods. To this, known amounts of cholesterol were added, which was obtained by removing plasma through centrifugation. The combined cholesterol level (i.e., original plus added) was determined from the fluorescence spectra with a calibration curve (Figure 6b). Table 1 shows the measured and known amounts of cholesterol in human serum. The recovery ratios (measured amounts/added amounts) were

97.4% and 107.9% for the two prepared samples at C_{cho} = 101 and 240 μM, respectively, indicating that this cholesterol biosensor can be used with real human blood samples. Although small deviations from 100% were observed, possibly reflecting interference from other biomaterials in human serum, the deviations were minimal.

Conclusions

In summary, a simple, highly sensitive, selective, rapid, and cost-effective cholesterol biosensor was developed based on the CD/Hb complex. The main mechanism of cholesterol sensing occurs via fluorescence enhancement of CD upon its interaction with cholesterol, which disrupts π-π interactions between CD and Hb that quench CD fluorescence. The CD/Hb complex provides a new platform for applications of CDs to biosensors, and this mechanism can be further applied to the development of other biosensor systems.

References

1. Voet, D., J.G. Voet, and C.W. Pratt, *Fundamentals of biochemistry : life at the molecular level*. Fourth edition ed. 2013: Hoboken, NJ : Wiley, ©2013.
2. Ma, H., *Cholesterol and Human Health.* Nature and Science, 2004. **4**: p. 5.
3. Nakaminami, T., S. Kuwabata, and H. Yoneyama, *Electrochemical Oxidation of Cholesterol Catalyzed by Cholesterol Oxidase with Use of an Artificial Electron Mediator.* Analytical Chemistry, 1997. **69**(13): p. 2367-2372.
4. Wong, W.W., et al., *An improved HPLC method to purify erythrocyte cholesterol for estimation of in vivo cholesterol synthesis using the deuterium method.* Applied Radiation and Isotopes, 1994. **45**(4): p. 529-533.
5. Singh, S.P., et al., *Cholesterol biosensor based on rf sputtered zinc oxide nanoporous thin film.* Applied Physics Letters, 2007. **91**(6): p. 063901.
6. Shenqi, W., L. Shipu, and Y. Yaoting, *Immobilization of Cholesterol Oxidase on Cellulose Acetate Membrane for Free Cholesterol Biosensor Development.* Artificial Cells, Blood Substitutes & Biotechnology, 2004. **32**(3): p. 413-425.
7. Kouassi, G.K., J. Irudayaraj, and G. McCarty, *Examination of Cholesterol oxidase attachment to magnetic nanoparticles.* Journal of Nanobiotechnology, 2005. **3**.
8. Vidal, J.-C., et al., *Amperometric cholesterol biosensors based on the electropolymerization of pyrrole and the electrocatalytic effect of Prussian-Blue layers helped with self-assembled monolayers.* Talanta, 2004. **64**(3): p. 655-664.
9. Torabi, S.-F., et al., *Covalent attachment of cholesterol oxidase and horseradish peroxidase on perlite through silanization: Activity, stability and co-immobilization.* Journal of Biotechnology, 2007. **131**(2): p. 111-120.
10. Noma, A. and K. Nakayama, *Polarographic method for rapid microdetermination of cholesterol with cholesterol esterase and cholesterol oxidase.* Clin Chem, 1976. **22**(3): p. 336-40.
11. P, A. and Demchenko, *Introduction to Fluorescence Sensing*. Biomedical Sciences. 2009: Springer Netherlands. XXVI, 590.
12. Wu, X.J. and M.M.F. Choi, *Hydrogel Network Entrapping Cholesterol Oxidase and Octadecylsilica for Optical Biosensing in Hydrophobic Organic or Aqueous Micelle Solvents.* Analytical Chemistry, 2003. **75**(16): p. 4019-4027.
13. Marazuela, M.D., et al., *Free cholesterol fiber-optic biosensor for serum samples with simplex optimization.* Biosensors and Bioelectronics, 1997. **12**(3): p. 233-240.
14. Kim, K.-E., T. Kim, and Y.-M. Sung, *Fluorescent cholesterol sensing using enzyme-modified CdSe/ZnS quantum dots.* Journal of Nanoparticle Research, 2012. **14**(10): p. 1-9.

15. Kirchner, C., et al., *Cytotoxicity of Colloidal CdSe and CdSe/ZnS Nanoparticles.* Nano Letters, 2005. **5**(2): p. 331-338.
16. Derfus, A.M., W.C.W. Chan, and S.N. Bhatia, *Probing the Cytotoxicity of Semiconductor Quantum Dots.* Nano Letters, 2004. **4**(1): p. 11-18.
17. Xu, X., et al., *Electrophoretic Analysis and Purification of Fluorescent Single-Walled Carbon Nanotube Fragments.* Journal of the American Chemical Society, 2004. **126**(40): p. 12736-12737.
18. Baker, S.N. and G.A. Baker, *Luminescent carbon nanodots: emergent nanolights.* Angew Chem Int Ed Engl, 2010. **49**(38): p. 6726-44.
19. Li, H., et al., *Carbon nanodots: synthesis, properties and applications.* Journal of Materials Chemistry, 2012. **22**(46): p. 24230-24253.
20. Bai, W., et al., *A carbon dots-based fluorescence turn-on method for DNA determination.* Anal Sci, 2011. **27**(3): p. 243-6.
21. Shen, P. and Y. Xia, *Synthesis-Modification Integration: One-Step Fabrication of Boronic Acid Functionalized Carbon Dots for Fluorescent Blood Sugar Sensing.* Analytical Chemistry, 2014. **86**(11): p. 5323-5329.
22. Qu, K., et al., *Carbon dots prepared by hydrothermal treatment of dopamine as an effective fluorescent sensing platform for the label-free detection of iron(III) ions and dopamine.* Chemistry, 2013. **19**(22): p. 7243-9.
23. Gu, J., et al., *Carbon dot cluster as an efficient "off-on" fluorescent probe to detect Au(III) and glutathione.* Biosens Bioelectron, 2015. **68**: p. 27-33.
24. Gao, Z., et al., *A carbon dot-based "off-on" fluorescent probe for highly selective and sensitive detection of phytic acid.* Biosens Bioelectron, 2015. **70**: p. 232-8.
25. Zhou, L., et al., *Carbon nanodots as fluorescence probes for rapid, sensitive, and label-free detection of Hg2+ and biothiols in complex matrices.* Chemical Communications, 2012. **48**(8): p. 1147-1149.
26. Kumar, D., et al., *Lipoidal Soft Hybrid Biocarriers of Supramolecular Construction for Drug Delivery.* ISRN Pharmaceutics, 2012. **2012**: p. 474830.
27. Qu, D., et al., *Formation mechanism and optimization of highly luminescent N-doped graphene quantum dots.* Scientific Reports, 2014. **4**: p. 5294.
28. Zeng, X., et al., *One-step fabrication of nitrogen-doped fluorescent nanoparticles from non-conjugated natural products and their temperature-sensing and bioimaging applications.* Sensing and Bio-Sensing Research, 2015. **3**: p. 18-23.
29. Dong, Y., et al., *Polyamine-functionalized carbon quantum dots for chemical sensing.* Carbon, 2012. **50**(8): p. 2810-2815.
30. Jin, S.H., et al., *Tuning the Photoluminescence of Graphene Quantum Dots through the Charge Transfer Effect of Functional Groups.* ACS Nano, 2013. **7**(2): p. 1239-1245.
31. Zhu, S., et al., *The photoluminescence mechanism in carbon dots (graphene quantum dots, carbon nanodots, and polymer dots): current state and future perspective.* Nano Research, 2015. **8**(2): p. 355-381.
32. Zhu, S., et al., *Highly photoluminescent carbon dots for multicolor patterning, sensors, and bioimaging.* Angew Chem Int Ed Engl, 2013. **52**(14): p. 3953-7.
33. Pan, D., et al., *Observation of pH-, solvent-, spin-, and excitation-dependent blue photoluminescence from carbon nanoparticles.* Chemical Communications, 2010. **46**(21): p. 3681-3683.
34. Luo, P.G., et al., *Carbon "quantum" dots for optical bioimaging.* Journal of Materials Chemistry B, 2013. **1**(16): p. 2116-2127.
35. Qu, Q., et al., *Development of a carbon quantum dots-based fluorescent Cu2+ probe suitable for living cell imaging.* Chemical Communications, 2012. **48**(44): p. 5473-5475.
36. Armbruster, D.A. and T. Pry, *Limit of Blank, Limit of Detection and Limit of Quantitation.* The Clinical Biochemist Reviews, 2008. **29**(Suppl 1): p. S49-S52.

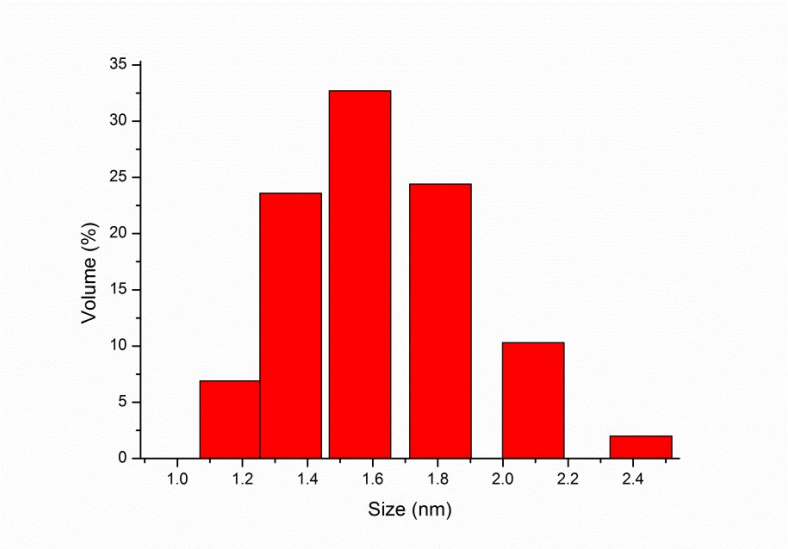

(a)

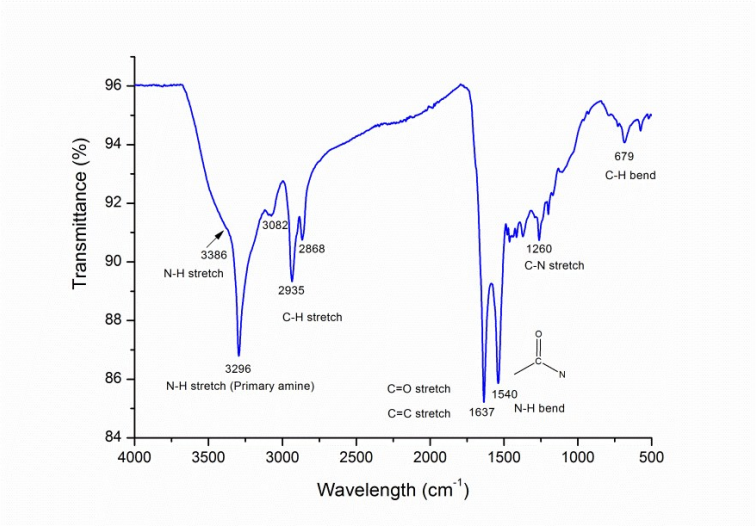

(b)

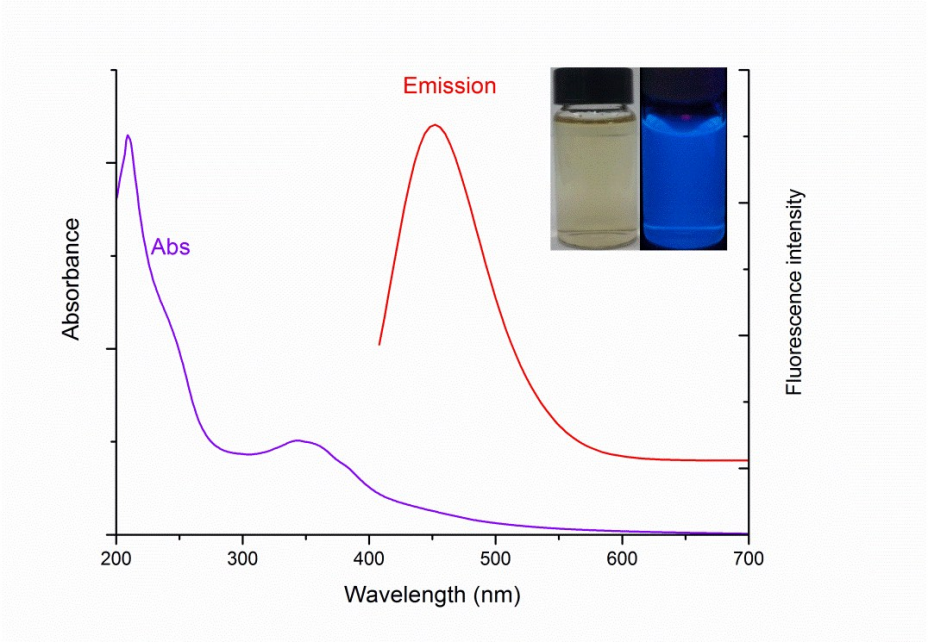

(c)

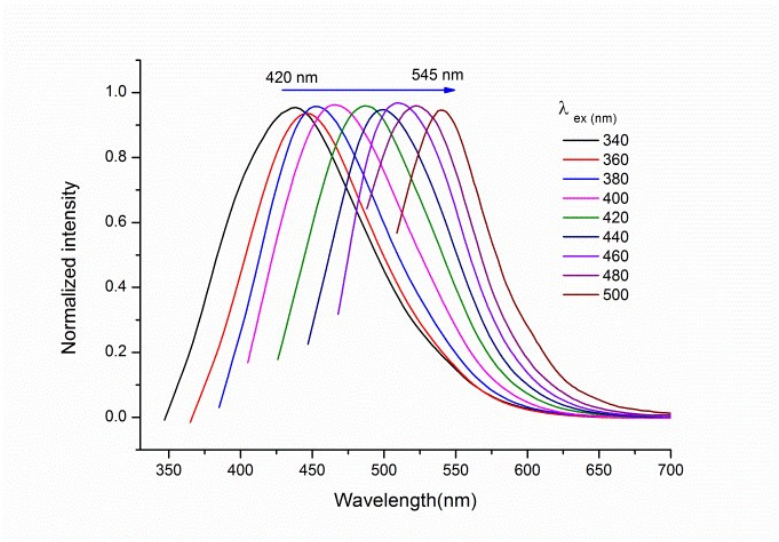

(d)

Figure 1. (a) Size distribution of CD was measured by DLS. (b) Surface chemical groups of CD were analyzed by FT-IR spectroscopy. (c) UV-Vis absorption and emission spectra (excited at 380 nm), and (d) normalized PL spectra excited at different wavelengths; the inset in (c) shows photographs of CD in aqueous solution (0.001 mg/mL) under white light (left) and UV light at 365 nm (right).

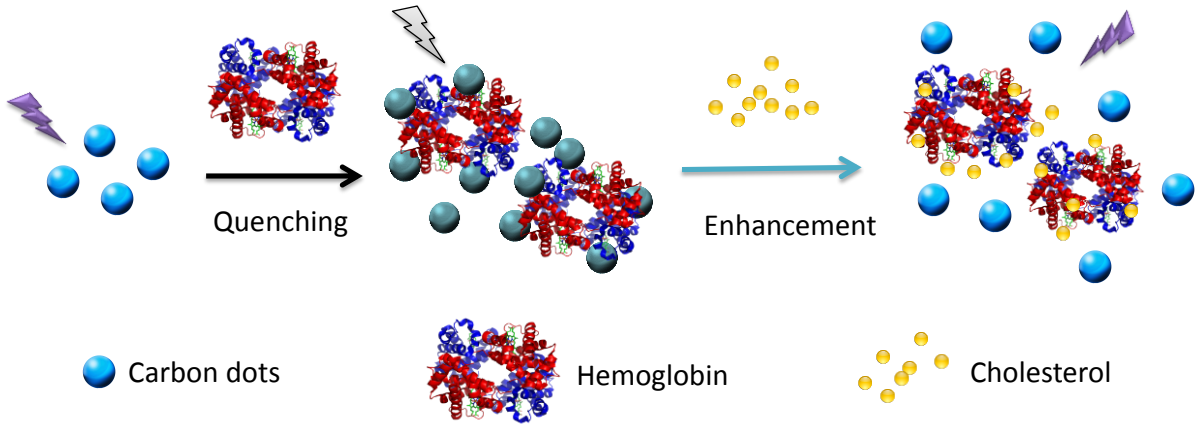

Scheme 1. Schematic illustration of fluorescence quenching of CD with Hb and enhancement with cholesterol.

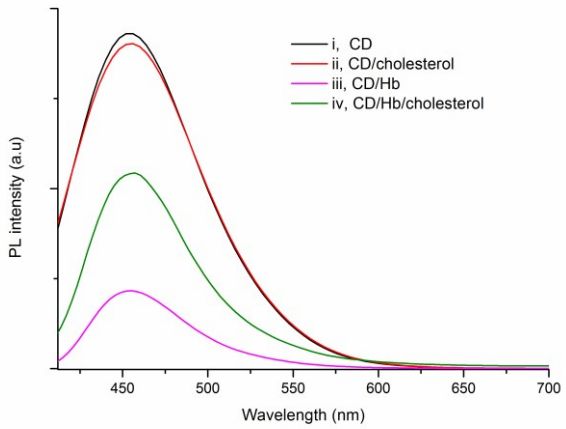

(a)

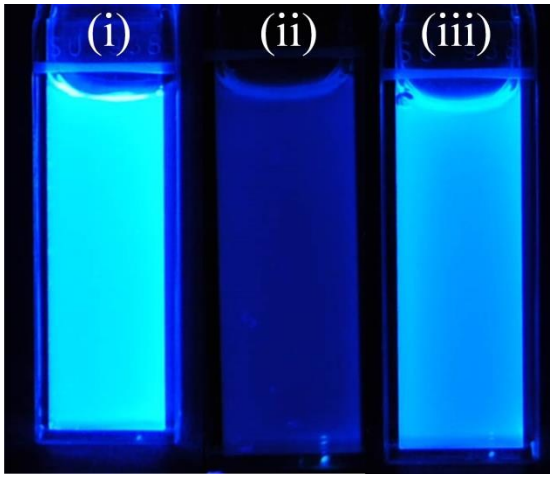

(b)

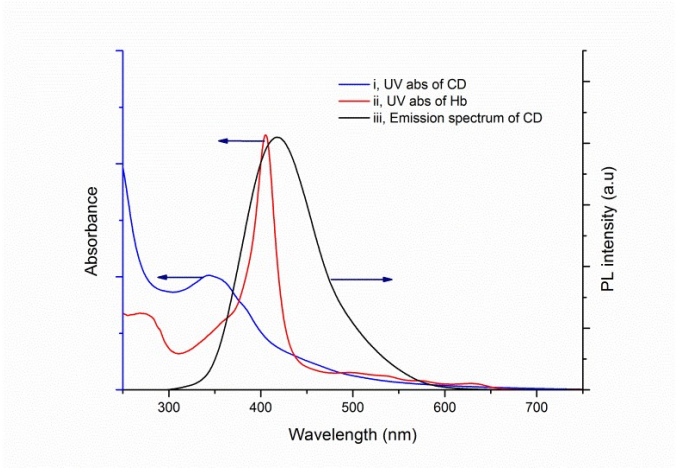

(c)

Figure 2. (a) Fluorescence spectra of (i) CD, (ii) CD/cholesterol, (iii) CD/Hb, (iv) CD/Hb/cholesterol excited at 380 nm. (b) Photographs of (i) CD, (ii) CD/Hb, and (iii) CD/Hb/cholesterol aqueous solutions under UV light (365 nm). (c) UV-Vis absorption spectra of (i) CD and (ii) Hb, and (iii) emission spectrum of CD excited at 380 nm, where the concentrations of aqueous CD, Hb, and cholesterol were 0.002 mg/mL, 6 μM, and 400 μM, respectively.

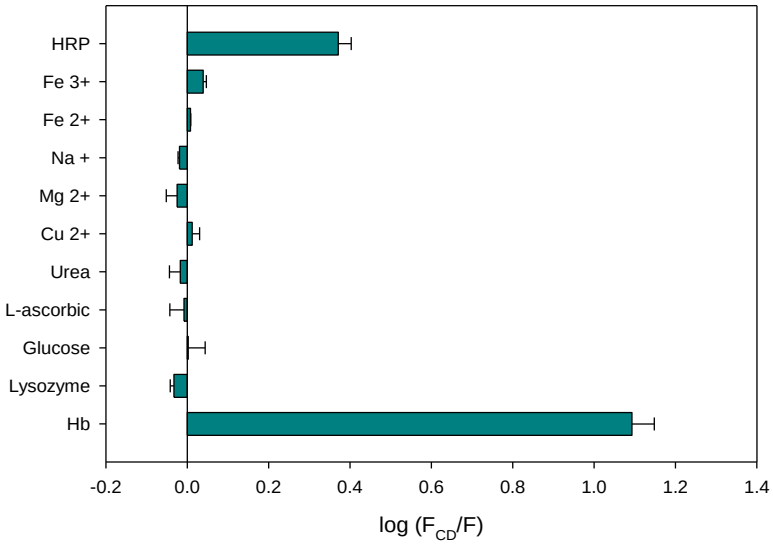

Figure 3. Log relative PL intensities (log (F_{CD}/F), where F_{CD} and F indicate PL intensities at 380 nm excitation before and after complexation, respectively), of aqueous Hb, HRP, lysozyme, L-ascorbic acid, urea, Cu^{2+}, Na^{+}, Fe^{2+}, Mg^{2+}, and glucose solutions at the same final concentration of 8 μM.

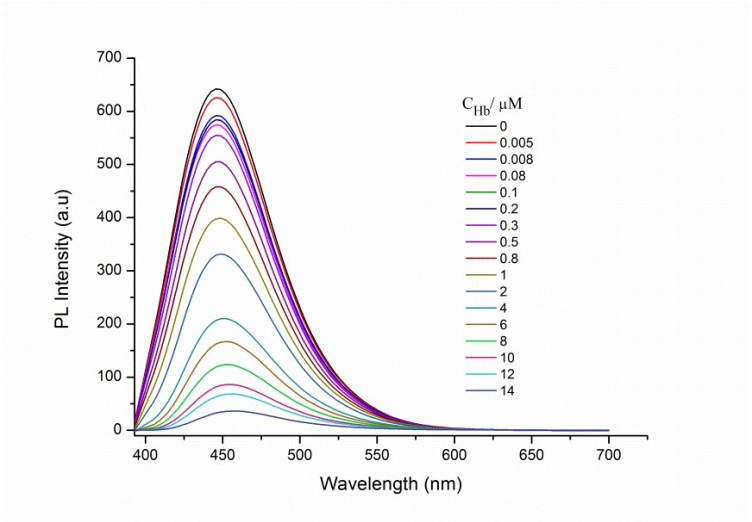

(a)

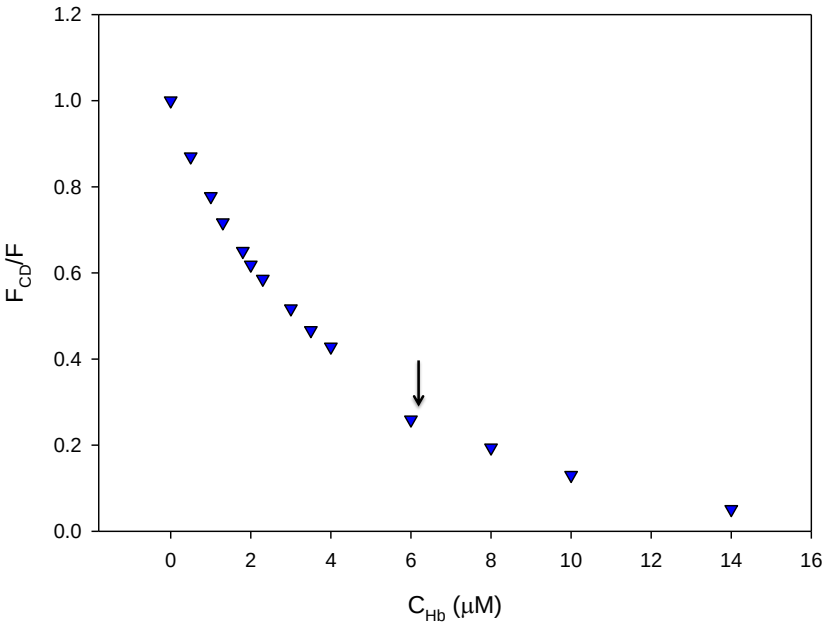

(b)

Figure 4. (a) Fluorescence spectra at different C_{Hb}s and (b) relative PL intensity of the CD/Hb complex ((F_{CD}/F), where F_{CD} and F indicate PL intensities before and after complexation, respectively) with increasing amounts of C_{Hb} at 380 nm excitation.

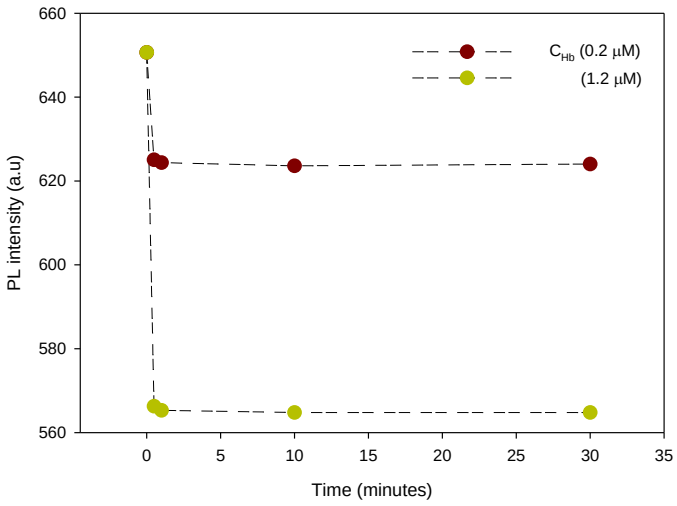

Figure 5. Time course of F_{CD}/F change after Hb was added to 0.002 mg/mL aqueous CD solutions to obtain C_{Hb} = 0.2 and 1.2 μM.

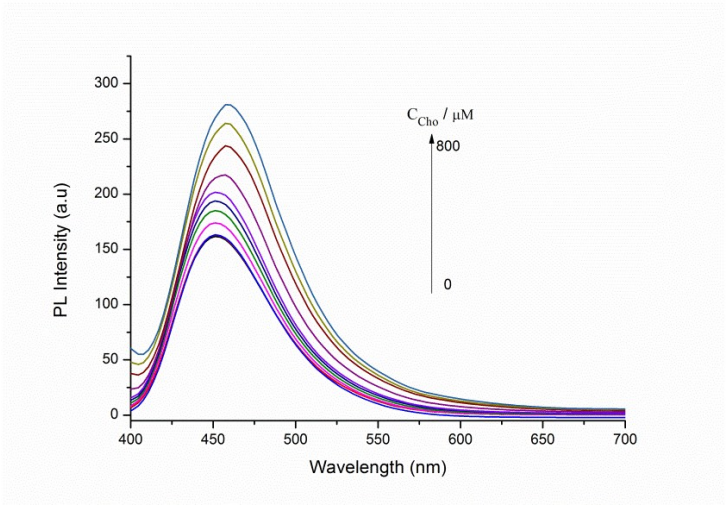

(a)

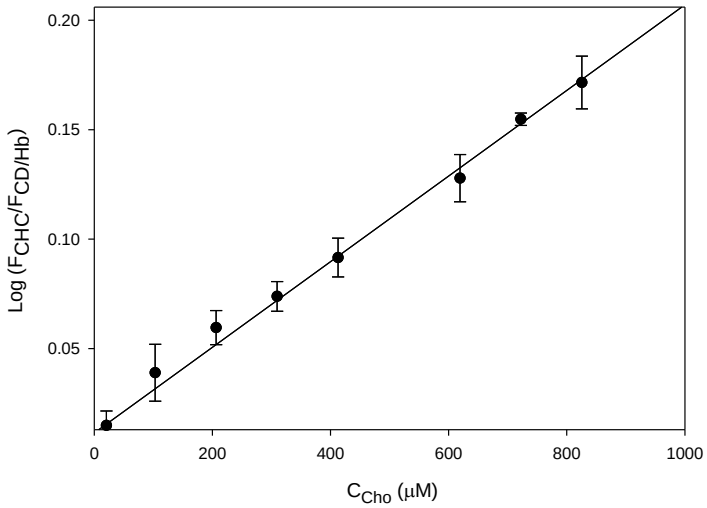

(b)

Figure 6. (a) Fluorescence spectra of CD/Hb/cholesterol solutions at different C_{cho} and (b) plot of log $F_{CHC}/F_{CD/Hb}$, where $F_{CD/Hb}$ and F_{CHC} are the PL intensities at 380 nm excitation before and after adding cholesterol, respectively, as a function of C_{cho}.

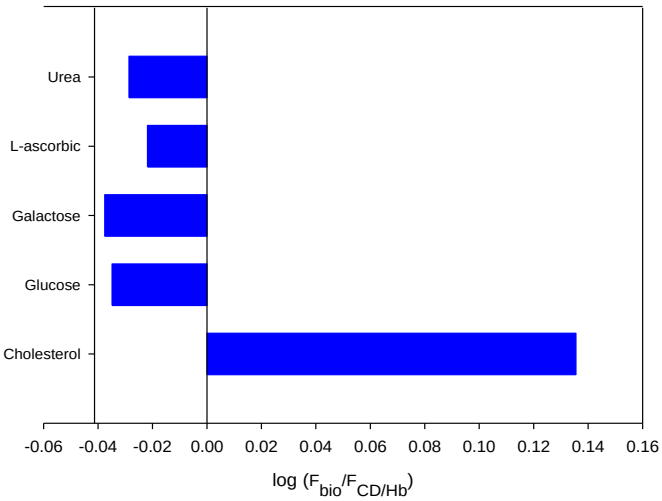

Figure 7. Plot of log ($F_{bio}/F_{CD/Hb}$), where $F_{CD/Hb}$ and F_{bio} indicate the PL intensities before and after adding biomaterials, respectively. Different biomaterials were used at the final concentration of 800 μM.

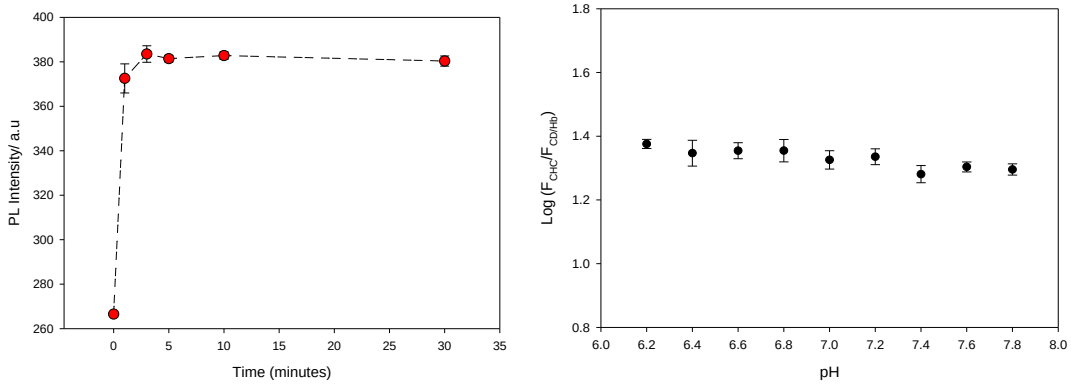

(a) (b)

Figure 8. (a) Fluorescence of the CD/Hb complex as a function of time after adding cholesterol. (b) The plot of the log ($F_{CHC}/F_{CD/Hb}$) as a function of pH, where $F_{CD/Hb}$ and F_{CHC} are the PL intensities before and after adding cholesterol, respectively. (C_{CD}: 0.002 mg/mL; C_{Hb}: 6 μM; C_{Cho}: 600 μM).

Table 1 Accuracy of measured cholesterol levels in human blood serum from intrinsic or extrinsic sources

Samples	Original cholesterol (Human serum) (μM)	Added cholesterol (μM)	Measured cholesterol (μM)	Recovery %	RSD (n = 3, %)
1	101	103	201	97.4	4.9
2	240	361	630	107.9	7.1

Note: Recovery = (Measured – Original)/ Added * 100%; RSD is the relative standard deviation